Volume 9, Issue 4, 2019, 4143 - 4149 ISSN 2069-5837

Biointerface Research in Applied Chemistry

www.BiointerfaceResearch.com

https://doi.org/10.33263/BRIAC94.143149

Original Research Article Open Access Journal

Received: 10.04.2019 / Revised: 22.07.2019 / Accepted: 04.08.2019 / Published on-line: 15.08.2019

Effect of nano metal oxides on the electronic properties of cellulose, chitosan and sodium alginate

Hend A. Ezzat [1], Maroof A. Hegazy [1], Nadra A. Nada [2], Medhat A. Ibrahim [3]

[1]National Research Institute of Astronomy and Geophysics (NRIAG), Helwan, Cairo, Egypt
[2]Physics Department, Faculty of Women for Arts, Science, and Education, Ain Shams University, 11757 Cairo, Egypt
[3]Spectroscopy Department, National Research Centre, 33 El-Bohouth St., 12622, Dokki, Giza, Egypt

*corresponding author e-mail address: ***medahmed6@yahoo.com***

ABSTRACT

Study of the effect of some Nano metal oxides MOs as CuO, OCu, ZnO and OZn on some bio-polymers as Cellulose, Chitosan and Sodium Alginate. Thus, model structure of two unit organic polymer Cellulose, Chitosan and Sodium Alginate and they with Nano MOs as CuO, OCu, ZnO and OZn are suggested. Density functional theory (DFT) conducted to study this effect atB3LYP/LANL2DZ. Computed HOMO-LUMO band gap energy(ΔE) and Total dipole moment (TDM) indicated that Cellulose and Chitosan affected by Nano MOs that TDM increased and ΔE decrease while Sodium Alginate has a slight change that has no effect on it. Also, calculated electrostatic potential (ESP) indicated that Cellulose and Chitosan affected by Nano MOs specially with CuO while Sodium Alginate has no effect.

Keywords: *Bio-polymers, Nano MOs, B3LYP/LANL2DZ, HOMO-LUMO band gap energy, TDM and ESP*.

1. INTRODUCTION

Cellulose is biopolymer which chemically described as β 1,4-linked d-glucose rings it is belonging to the family of polysaccharides [1]. It is the most abundant: recyclable; biocompatible; renewable and biodegradable polysaccharides [2,3]. Physically, it is a crude form known as hydrophilic, odorless and tasteless in nature [4]. Cellulose show emerging applications in paper and cardboard industry due to its unique physical and chemical properties [5]. Nanocellulose which is extracting from cellulose show amazing enhancement in cellulose properties [6]. Chitosan is another member of polysaccharides has almost the same features of cellulose as well as other polysaccharides. It is chemically co-polymer of N-glucosamine and N-acetyl-glucosamine linked by β-(1′4)-glycosidic bonds. It is derived from the N-acetylation of chitin in hot alkaline media [7-8]. Furthermore, it has been widely chemical modified. Such modifications make it meets various biological and medical needs due to its active functional groups [9-12]. Sodium alginate is also belonging to the class carbohydrate biopolymer of formula $(C_6H_7Na_{1/2}O_6)_n$, extracted from brown algae, such as Laminaria or Fucus, that widely used in the food industries and textures. It has wide range of applications according to unique properties [13-16]. Cellulose; chitosan and sodium alginate are continuing to be a topic of extensive research work [17-22]. Throughout chemical enhancements in their properties paves the way toward further applications. This in turn must be followed with a technique to monitor the changes in their electronic properties. Molecular modeling dedicated to act like this not only for the studied structures but also for the polysaccharides [23-26]. Generally molecular modeling is widely applied to study structural, thermal and vibrational features of many systems and molecules [27-29].

Based on these considerations molecular modeling at B3LYP/LANL2DZ is utilized to study the effect Nano Metal Oxides on the Electronic Properties of Cellulose, Chitosan and Sodium Alginate respectively.

2. MATERIALS AND METHODS

Computational Details.

Model structures of two units of bio-polymers: Cellulose, Chitosan and sodium Alginate and the same bio-polymers with Nano MOs calculated by using GAUSSIAN09 program [30] at Spectroscopy Department, National Research Centre, Egypt. All Model structures calculated by using DFT theory at B3LYP level [31-33] using LANL2DZ basis set. HOMO-LUMO band gap energy and TDM are also computed using the same level of theory. ESP also computed for the same model structures as contour and 3D total surface action.

3. RESULTS

Model structures were performed to study effect of Nano MOs as: CuO, OCu, ZnO and OZn on some bio-polymers as: Cellulose, Chitosan and sodium Alginate. Model structures of two units of bio-polymers: Cellulose, Chitosan and sodium Alginate were supposed as shown in figure 1(a), 2(a) and 3(a): respectively. Also models for two units of natrual polymers: Cellulose, Chitosan and sodium Alginate with Nano MOs;CuO, OCu, ZnO and OZn were proposed as in figure 1(c, e and i), 2(c, e and i) and 3(c, e and i) respectively. HOMO-LUMO band gap energy and

TDM are also computed for all model structures using DFT theory at B3LYP level using LANL2DZ basis set.

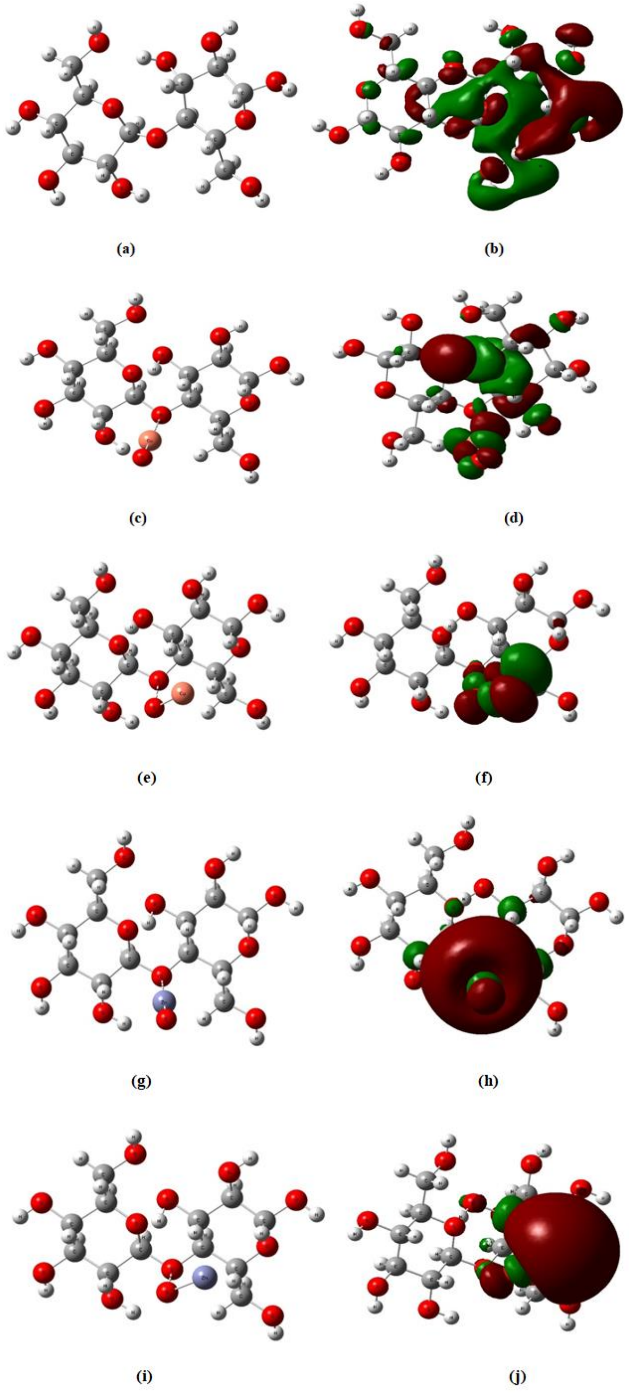

Figure 1. Model structures of two units of Cellulose and Cellulose with metal oxide and its HOMO-LUMO band gap energy optimized at B3LYP/LANL2DZ basis set as (a) Cellulose, (b) HOMO-LUMO of Cellulose (c) Cellulose + CuO;, (d) HOMO-LUMO of Cellulose +CuO (e) Cellulose + OCu, (f) HOMO-LUMO of Cellulose + OCu (g) Cellulose + ZnO, (h) HOMO-LUMO of Cellulose + ZnO (i) Cellulose + OZn, (j) HOMO-LUMO of Cellulose + OZn.

Firstly, Cellulose and Cellulose with Nano MOs: CuO, OCu, ZnO and OZn optimized structure and change in their HOMO-LUMO band gap energy were computed at B3LYP / LANL2DZas shown in figure 1.Table 1 shown change in HOMO-LUMO band gap energy ΔE and TDM for cellulose with Nano MOs: CuO, OCu, ZnO and OZn. HOMO-LUMO band gap energy ΔE and TDM changed for Cellulose with CuO from 3.6578 to 0.6376 eV and from 6.2868 to 18.6935 Debye respectively. TDM for Cellulose with CuO increased while HOMO-LUMO band gap energy ΔE decreased that means reactivity of cellulose increased with CuO. Also, for Cellulose with OCu TDM changed to3.2394 Debye while HOMO-LUMO band gap energy ΔE changed to 0.6027eV that TDM decrease and ΔE decrease which means that reactivity has no change. Then, for Cellulose with ZnO HOMO-LUMO band gap energy ΔE and TDM changed to 0.8147 eV and to 8.9236Debye respectively that TDM increase while ΔE decreases that reactivity improved slightly. As previous Cellulose with OZn also TDM decreased to 2.4371 Debye while HOMO-LUMO band gap energy ΔE also decreased to 0.8814 eV which means that the reactivity also has no change.

Table 1. Calculated HOMO-LUMO band gap energy ΔE (eV) and total dipole moment TDM (Debye) Using B3LYP/LANL2DZ for Cellulose, Cellulose+CuO, Cellulose+OCu, Cellulose+ZnO and Cellulose+OZn.

Structure	TDM	ΔE
Cellulose	6.2868	3.6578
Cellulose + CuO	18.6935	0.6376
Cellulose + OCu	3.2394	0.6027
Cellulose + ZnO	8.9236	0.8147
Cellulose + OZn	2.4371	0.8814

Secondly, Chitosan and Chitosan with Nano MOs: CuO, OCu, ZnO and OZn optimized structure and their HOMO-LUMO band gap energy also were calculated at B3LYP / LANL2DZ as shown in figure 2. Change in HOMO-LUMO band gap energy ΔE and TDM for Chitosan with Nano MOs: CuO, OCu, ZnO and OZn shown in table 2. HOMO-LUMO band gap energy ΔE and TDM for Chitosan with CuO changed from 2.8891to 0.5148eV and from 3.32040 to 16.8125 Debye respectively where TDM increased while HOMO-LUMO band gap energy ΔE decreased that means reactivity of Chitosan increased with CuO. Also, for Chitosan with OCu TDM changed to 16.7206 Debye at the same time HOMO-LUMO band gap energy ΔE changed to 0.9565 eV that TDM increased and ΔE decrease which means that reactivity increased for OCu also. Then, for Chitosan with ZnO HOMO-LUMO band gap energy ΔE and TDM changed to 0.6025 eV and to 9.6583Debye respectively that TDM increase while ΔE decreases that reactivity improved slightly. As previous Chitosan with OZn also TDM increased to 13.6988Debye while HOMO-LUMO band gap energy ΔE also decreased to 0.6261 eV that the reactivity also changes positively.

Table 2. Calculated HOMO-LUMO band gap energy ΔE (eV) and total dipole moment TDM (Debye) Using B3LYP/LANL2DZ for Chitosan, Chitosan +CuO, Chitosan +OCu, Chitosan +ZnO and Chitosan +OZn.

Structure	TDM	ΔE
Chitosan	3.32040	2.8891
Chitosan + CuO	16.8125	0.5148
Chitosan + OCu	16.7206	0.9565
Chitosan + ZnO	9.6583	0.6025
Chitosan + OZn	13.6988	0.6261

Furthermore, Sodium Alginate and Sodium Alginate with Nano MOs: CuO, OCu, ZnO and OZn also optimized and their HOMO-LUMO band gap energy also were calculated at B3LYP / LANL2DZ as shown in figure 3. Change in HOMO-LUMO band gap energy ΔE and TDM for Sodium Alginate with Nano MOs: CuO, OCu, ZnO and OZn showed in table 3. For Sodium Alginate with CuO TDM changed from 13.0524 to 12.7533Debye and ΔE changed from 0.7083 to 1.0368 eV that TDM decrease and ΔE increase which means that reactivity changes negatively. HOMO-LUMO band gap energy ΔE and TDM for Sodium Alginate with

OCu changed to 0.7973 eV and to 13.3502 Debye respectively where TDM slightly increased while HOMO-LUMO band gap energy ΔE slightly decreased that means reactivity of Sodium Alginate with CuO has no change. Also, HOMO-LUMO band gap energy ΔE and TDM for Sodium Alginate with ZnO and OZn were changed to 0.9445 and 0.7029 eV and to 17.5735 and 18.2395 Debye respectively which also means that there have no change in reactivity.

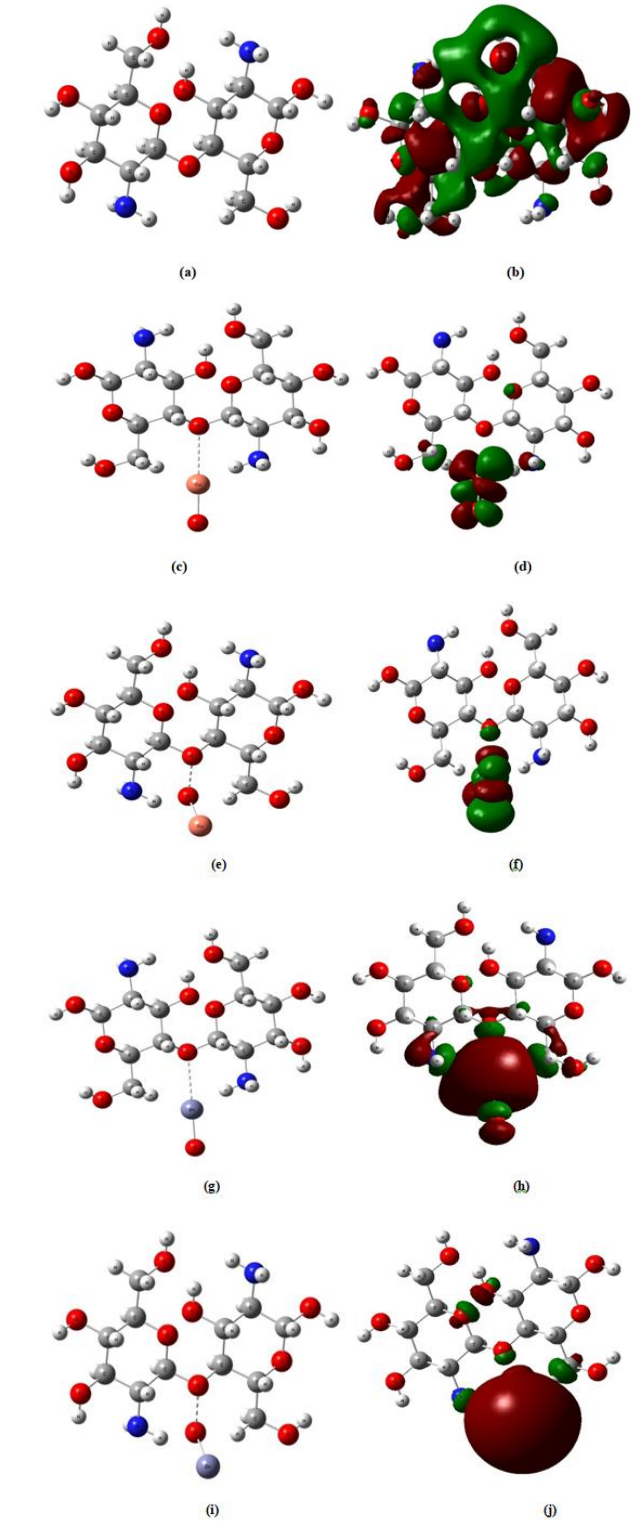

Figure 2. Model structures of two units of Chitosan and Chitosan with metal oxid and its HOMO-LUMO band gap energy optimized at B3LYP/LANL2DZ basis set as (a) Chitosan,(b) HOMO-LUMO of Chitosan (c) Chitosan + CuO , (d) HOMO-LUMO of Chitosan +CuO (e) Chitosan + OCu**;,** (f) HOMO-LUMO of Chitosan + OCu (g) Chitosan + ZnO, (h) HOMO-LUMO of Chitosan + ZnO (i) Chitosan + OZnl ,(j) HOMO-LUMO of Chitosan + OZn.

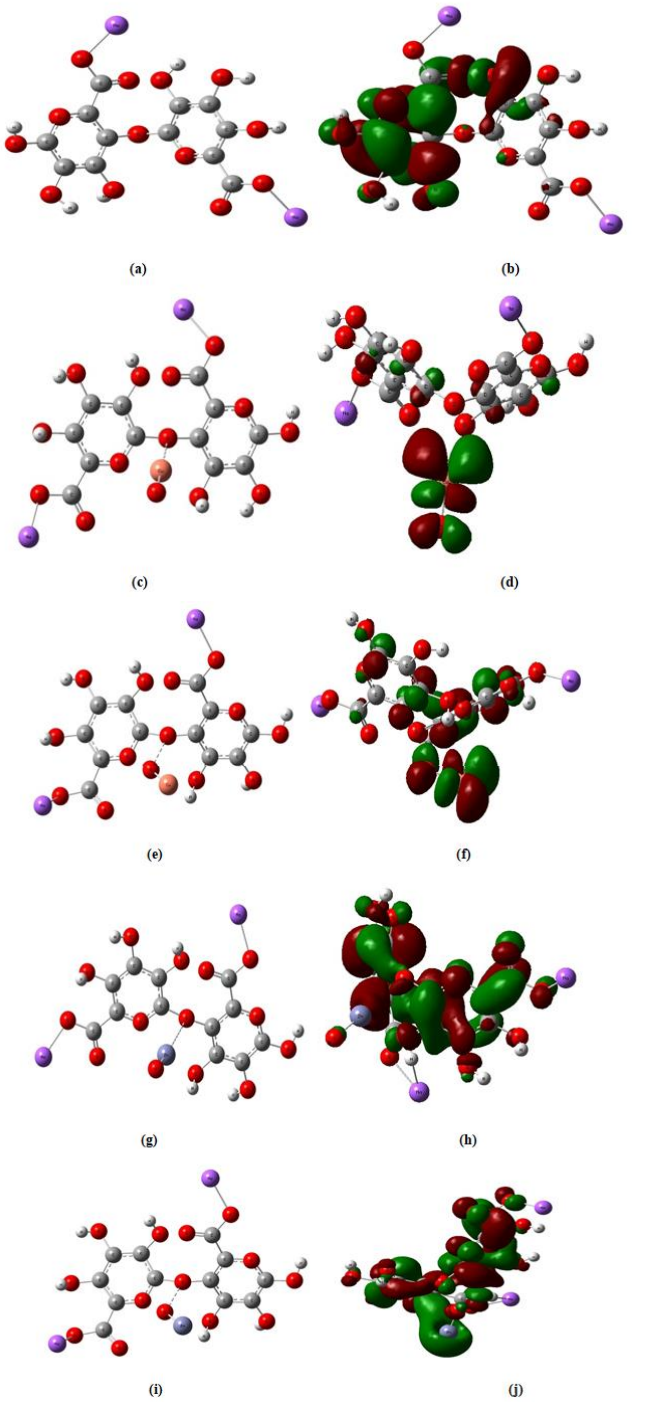

Figure 3. Model structures of two units of Sodium Alginate and Sodium Alginate with metal oxid and its HOMO-LUMO band gap energy optimized at B3LYP/LANL2DZ basis set as (a) Sodium Alginate, (b) HOMO-LUMO of Sodium Alginate, (c) Sodium Alginate +CuO, (d) HOMO-LUMO of Sodium Alginate +CuO, (e) Sodium Alginate + OCu, (f) HOMO-LUMO of Sodium Alginate + OCu, (g) Sodium Alginate+ ZnO, (h) HOMO-LUMO of Sodium Alginate + ZnO, (i) Sodium Alginate + OZn, (j) HOMO-LUMO of Sodium Alginate+ OZn

Table 3. Calculated HOMO-LUMO band gap energy ΔE (eV) and total dipole moment TDM (Debye) Using B3LYP/LANL2DZ for Sodium Alginate,Sodium Alginate +CuO, Sodium Alginate +OCu, Sodium Alginate +ZnO and Sodium Alginate +OZn.

Structure	TDM	ΔE
Sodium Alginate	13.0524	0.7083
Sodium Alginate + CuO	12.7533	1.0368
Sodium Alginate + OCu	13.3502	0.7973
Sodium Alginate + ZnO	17.5735	0.9445
Sodium Alginate + OZn	18.2395	0.7029

For further study also, we calculate ESP for Cellulose, Chitosan and Sodium Alginate with Nano MOs: CuO, OCu, ZnO and OZn on the same level of theory as previous. ESP represents the measure of nearby charges, nuclei and electrons strength at a specific position. The ESP data interpret by a color spectrum ranged as Red <orange <yellow <green<blue. The color variation conveys the varying in ESP intensities that red represents the lowest ESP value and blue represent the highest ESP value. ESP calculation is important to find out the reactive site of the molecule that has an affinity to interact with another particle.

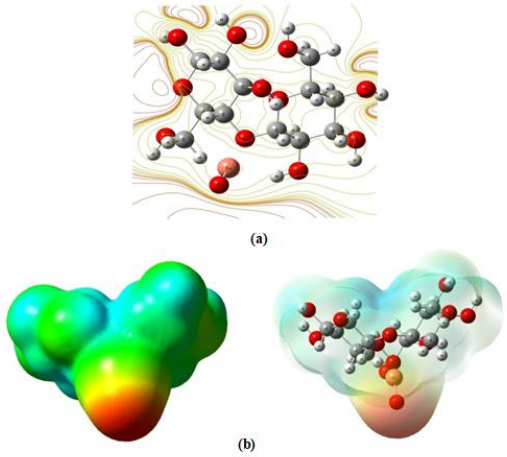

Figure 4. Electrostatic potential of Cellulose + CuO (a) as contour, (b) as 3D total surface.

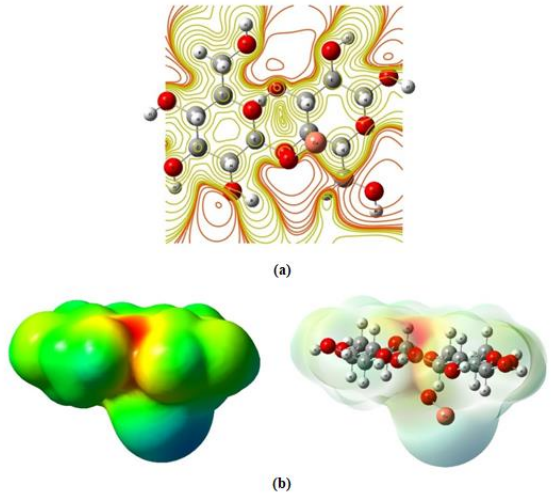

Figure 5. Electrostatic potential of Cellulose + OCu (a) as contour, (b) as 3D total surface.

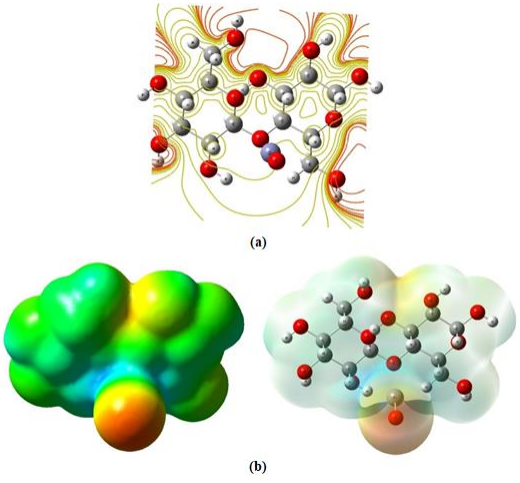

Figure 6. Electrostatic potential of Cellulose + ZnO (a) as contour, (b) as 3D total surface.

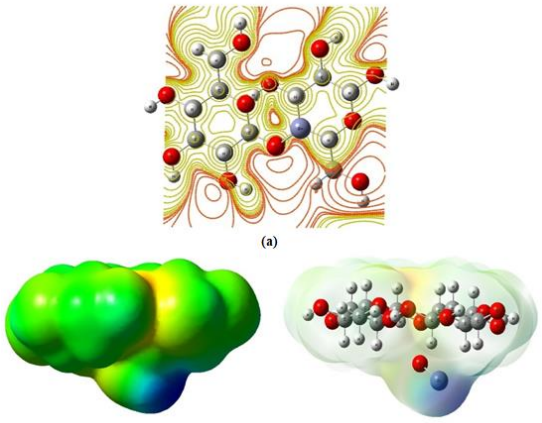

Figure 7. Electrostatic potential of Cellulose +OZn (a) as contour, (b) as 3D total surface.

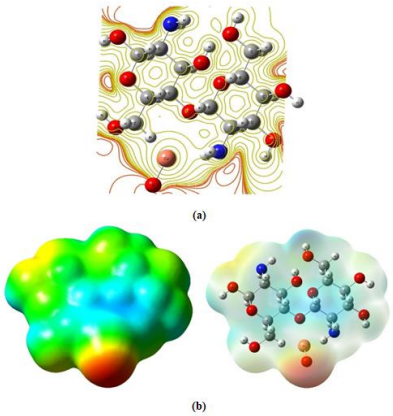

Figure 8. Electrostatic potential of Chitosan+CuO (a) as contour, (b) as 3D total surface.

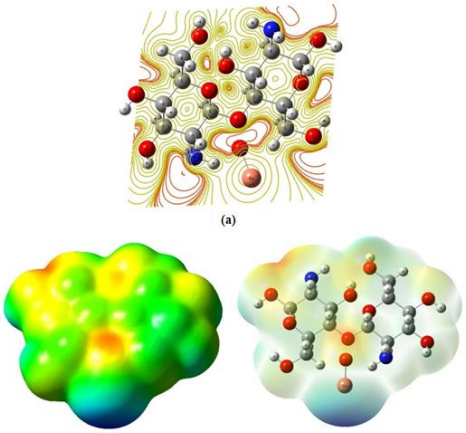

Figure 9. Electrostatic potential of Chitosan+OCu (a) as contour, (b) as 3D total surface.

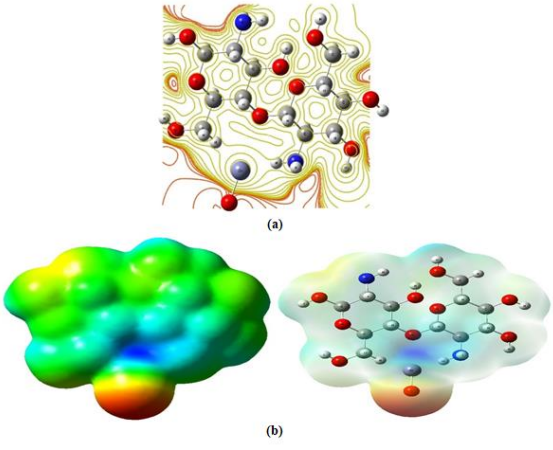

Figure 10. Electrostatic potential of Chitosan+ZnO (a) as contour, (b) as 3D total surface.

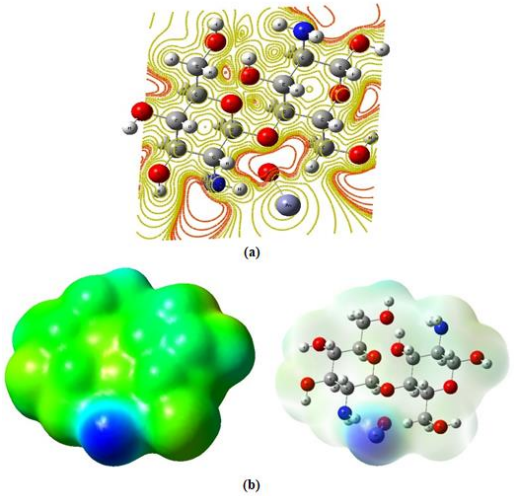

Figure 11. Electrostatic potential of Chitosan+OZn (a) as contour, (b) as 3D total surface.

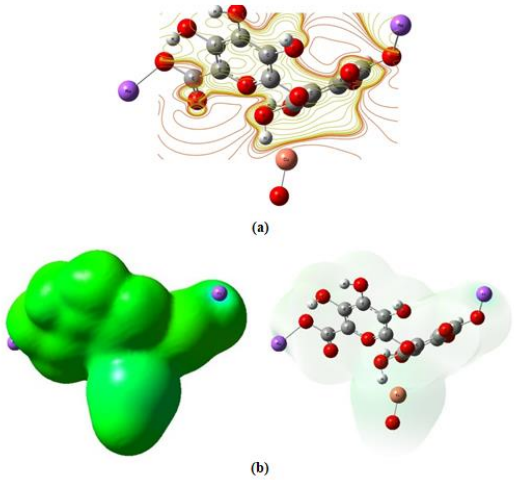

Figure 12. Electrostatic potential of Sodium Alginate+CuO (a) as contour, (b) as 3D total surface.

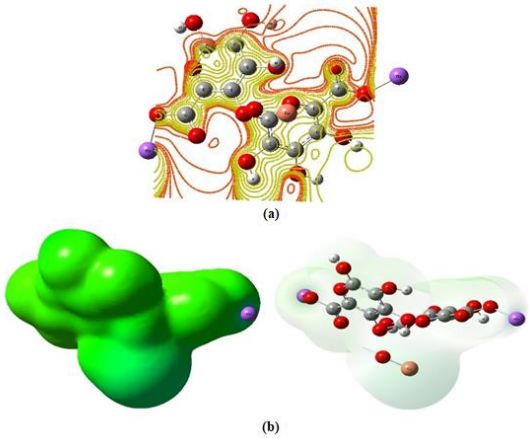

Figure 13. Electrostatic potential of Sodium Alginate+OCu (a) as contour, (b) as 3D total surface.

As shown in fig 4, 5, 6 and 7 ESP for Cellulose with Nano MOs: CuO, OCu, ZnO and OZn the regions of low potential red represent the abundance of electrons and the regions of high potential blue represent the absence of electrons. Oxygen atoms rounded by electron density more than Copper and Zinc atoms so the spherical region rounded Oxygen atom have a red color for Cellulose with Nano MOs: CuO and ZnO while the spherical region rounded Copper and Zinc atoms have blue color for Cellulose with Nano MOs: OCu and OZn. Also, ESP for Chitosan with Nano MOs: CuO, OCu, ZnO and OZn the spherical region rounded Oxygen atom have a red color while the spherical region rounded Copper and Zinc atoms have a blue color shown in fig 8, 9, 10 and 11. Red region represents the lowest electrostatic potential and greatest electronegativity which means that it have a high opportunity to interact with others. For Sodium Alginate with Nano MOs: CuO, OCu, ZnO and OZn as in fig 12, 13, 14 and 15 intermediary colors between red and blue represent less electronegativity difference which means that there is no chance to interact with others. Finally from all ESP results, Cellulose with Nano MOs: CuO and ZnO and Chitosan with Nano MOs: CuO and ZnO is the most reactive structures which have the great opportunity to interact with others while all Sodium Alginate with Nano MOs: CuO, OCu, ZnO and OZn have low electronegativity difference and its chance to be reactive is too low.

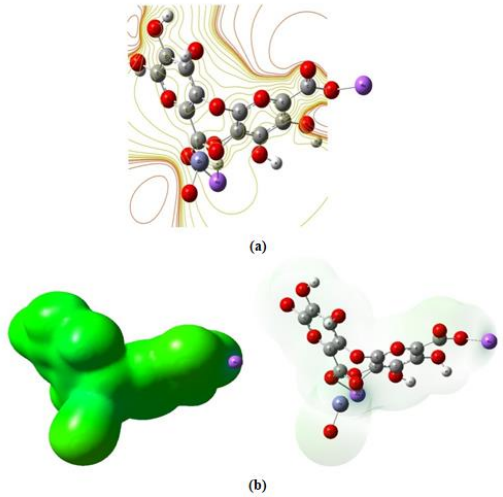

Figure 14. Electrostatic potential of Sodium Alginate+ZnO (a) as contour, b) as 3D total surface.

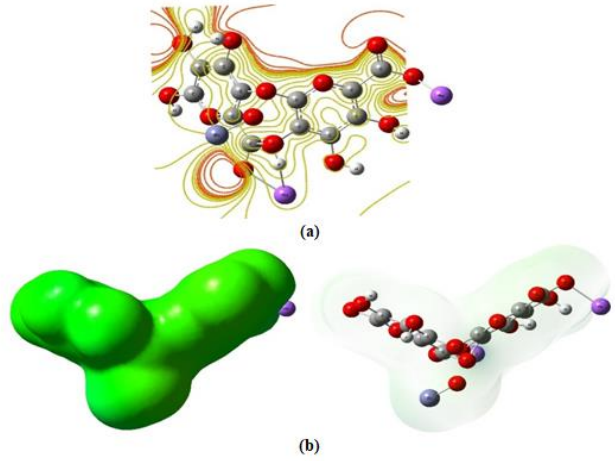

Figure 15. Electrostatic potential of Sodium Alginate+OZn (a) as contour (b) as 3D total surface.

4. CONCLUSIONS

From all studied structures Cellulose, Chitosan and Sodium Alginate with Nano MOs: CuO, OCu, ZnO and OZn, HOMO-LUMO band gap energy ΔE and TDM results indicated that HOMO-LUMO band gap energy ΔE and TDM changed for Cellulose with CuO from 3.6578 to 0.6376 eV and from 6.2868 to 18.6935 Debye respectively. TDM for Cellulose with CuO

increased while HOMO-LUMO band gap energy ΔE decreased that means reactivity of cellulose increased with CuO and for Cellulose with ZnO HOMO-LUMO band gap energy ΔE and TDM changed to 0.8147 eV and to 8.9236 Debye respectively that TDM increase while ΔE decrease that reactivity improved slightly. Also, HOMO-LUMO band gap energyΔE and TDM for Chitosan with CuO changed from 2.8891 to 0.5148 eV and from 3.32040 to 16.8125 Debye respectively that TDM increased while HOMO-LUMO band gap energy ΔE decreased that means reactivity of Chitosan increased with CuO and for Chitosan with ZnO HOMO-LUMO band gap energy ΔE and TDM changed to 0.6025 eV and to 9.6583Debye respectively that TDM increase while ΔE decrease that reactivity improved slightly. Furthermore, Sodium Alginate with Nano MOs: CuO, OCu, ZnO and OZn have no change in reactivity.

Accordingly, from all ESP results, Cellulose with Nano MOs: CuO and ZnO and Chitosan with Nano MOs: CuO and ZnO are the most reactive structures which have the great opportunity to interact with others while all Sodium Alginate with Nano MOs: CuO, OCu, ZnO and OZn have low electronegativity difference and its chance to be reactive is too low.

5. REFERENCES

1. Lefebvre, J.; Gray, D.G. AFM of adsorbed polyelectrolytes on cellulose I surfaces spin-coated on silicon wafers. *Cellulose* **2005**, *12*, 127-134, https://doi.org/10.1007/s10570-004-1574-0.
2. Crawford, R.L. *Lignin Biodegradation and Transformation*. John Wiley and Sons, New York, 1981; pp.154.
3. Updegraff, D.M. Semimicro determination of cellulose inbiological materials. *Analytical Biochemistry* **1969**, *32*, 420-424, https://doi.org/10.1016/S0003-2697(69)80009-6.
4. Charles, A.B. *Vacuum Deposition Onto Webs, Films, and Foils*. William Andrew, Elsevier, 2007; pp. 8155.
5. Dufresne, A. Polysaccharide nano crystal reinforced nanocomposites. *Canadian Journal of Chemistry* **2008**, *86*, 484-494, https://doi.org/10.1139/v07-152.
6. Dufresne, A. Nanocellulose: a new ageless bionanomaterial. *Materials today* **2013**, *16*, 220-227, https://doi.org/10.1016/j.mattod.2013.06.004.
7. Ashrafi, H.; Azadi, A. Chitosan-based hydrogel nanoparticle amazing behaviors during transmission electron microscopy. *International Journal of Biological Macromolecules* **2015**, *84*, 31-34, https://doi.org/10.1016/j.ijbiomac.2015.11.089.
8. Saboktakin, M.R.; Tabatabaie, R.M.; Maharramov, A.; Ramazanov, M.A. Synthesis and characterization of pH-dependent glycol chitosan and dextran sulfate nanoparticles for effective brain cancer treatment. *International Journal of Biological Macromolecules* **2011**, *49*, 747-751, https://doi.org/10.1016/j.ijbiomac.2011.07.006.
9. Sahariah, P.; Másson, M. Antimicrobial chitosan and chitosan derivatives: a review of the structure-activity Relationship. *Biomacromolecules* **2017**, *18*, 3846-3868, https://doi.org/10.1021/acs.biomac.7b01058.
10. El, K.H.; Belaabed, R.; Addaou, A.; Laajeb, A.; Lahsini, A. Extraction chemical modification and characterization of chitin and chitosan. *International Journal of Biological Macromolecules* **2018**, *120*, 1181-1189, https://doi.org/10.1016/j.ijbiomac.2018.08.139.
11. Lin, T.; Liu, E.; He, H.; Shin, M.C.; Moon, C.; Yang, V.C.; Huang, Y. Nose-to-brain delivery of macromolecules mediated by cell-penetrating peptides. *Acta Pharmaceutica Sinica B* **2016**, *6*, 352-358, https://doi.org/10.1016/j.apsb.2016.04.001.
12. Yu, S.; Xu, X.; Feng, J.; Liu, M.; Hu, K. Chitosan and chitosan coating nanoparticles for the treatment of brain disease. *International Journal of Pharmaceutics* **2019**, *560*, 282-293, https://doi.org/10.1016/j.ijpharm.2019.02.012,
13. Rioux, L.E.; Turgeon, S.L.; Beaulieu, M. Characterization of polysaccharides extracted from brown seaweeds. *Carbohydrate Polymers* **2007**, *69*, 530-537, https://doi.org/10.1016/j.carbpol.2007.01.009.
14. Gomez, C.G.; Pérez Lambrecht, M.V.; Lozano, J.E.; Rinaudo, M.; Villar, M.A. Influence of the extraction–purification conditions on final properties of alginates obtained from brown algae (Macrocystis pyrifera). *International Journal of Biological Macromolecules* **2009**, *44*, 365-371, https://doi.org/10.1016/j.ijbiomac.2009.02.005.
15. Kovalenko, I.; Zdyrko, B.; Magasinski, A.; Hertzberg, B.; Milicev, Z. A major constituent of brown algae for use in high-capacity Li-Ion batteries. *Science* **2011**, *334*, 75-79.
16. Jmiai, A.; El Ibrahimi, B.; Tara, A.; El Issami, S.; Jbara, O.; Bazzi, L. Alginate biopolymer as green corrosion inhibitor for copper in 1 M hydrochloric acid: Experimental and theoretical approaches. *Journal of Molecular Structure* **2018**, *1157*, 408-417, https://doi.org/10.1016/j.molstruc.2017.12.060.
17. Laffleur, F.; Röttges, S. Mucoadhesive approach for buccal application: Preactivated chitosan. *European Polymer Journal* **2019**, *113*, 60-66, https://doi.org/10.1016/j.eurpolymj.2019.01.049.
18. Kazi, G.A.S.; Yamamoto, O. Effectiveness of the sodium alginate as surgical sealant materials. *Wound Medicine* **2019**, *24*, 18-23, https://doi.org/10.1016/j.wndm.2019.02.001.
19. Wang, X.; Zhang, Y.; Liang, H.; Zhou, X.; Luo, Y. Effectiveness of the sodium alginate as surgical sealant materials. *Carbohydrate Polymers* **2019**, *208*, 391-397.
20. Vanitjinda, G.; Nimchua, T.; Sukyai, P. Effect of xylanase-assisted pretreatment on the properties of cellulose and regenerated cellulose films from sugarcane bagasse. *International Journal of Biological Macromolecules* **2019**, *122*, 503-516, https://doi.org/10.1016/j.ijbiomac.2018.10.191.
21. Khalid, A.; Khan, R.; Ul-Islam, M.; Khn, T.; Wahid, F. Bacterial cellulose-zinc oxide nanocomposites as a novel dressing system for burn wounds. *Carbohydrate Polymers* **2017**, *164*, 214-221, https://doi.org/10.1016/j.carbpol.2017.01.061.
22. Lefatshe, K.; Muiva, C.M.; Kebaabetswe, L.P. Extraction of nanocellulose and in-situ casting of ZnO/cellulose nanocomposite with enhanced photocatalytic and antibacterial activity. *Carbohydrate Polymers* **2017**, *164*, 301-308, https://doi.org/10.1016/j.carbpol.2017.02.020.
23. Ammar, N.S.; Elhaes, H.; Ibrahim, H.S.; El-hotaby, W.; Ibrahim, M.A. A Novel Structure for Removal of Pollutants from Wastewater. *Spectrochimica Acta Part A* **2014,** *121*, 216-223, https://doi.org/10.1016/j.saa.2013.10.063.
24. Abdel-Gawad, A.A.; Ibrahim, M. Computational Studies of The Interaction of Chitosan Nanoparticles and αB-Crystallin. *BioNanoScience* **2013**, *3*, 302-311, https://doi.org/10.1007/s12668-013-0096-3.
25. Omar, A.; El-Sayed, E.M.; Talaat, M.S.; Ibrahim, M. DNA Hybridization on Chitosan-Functionalized Silicon Substrat. *Medicinal Chemistry* **2016,** *12*, 464-471.
26. Galal, A.M.F.; Atta, D.; Abouelsayed, A.; Ibrahim, M.A.; Hanna, A.G. Configuration and Molecular Structure of 5-Chloro-N-(4-sulfamoylbenzyl) Salicylamide Derivatives.

Spectrochimica Acta A **2019**, *214*, 476–486, https://doi.org/10.1016/j.saa.2019.02.070.
27. Mahmoud, A.; Osman, O.; Elhaes, H.; Ferretti, M.; Fakhry, A.; Ibrahim, M.A. Computational Analyses for the Interaction Between Aspartic Acid and Iron. *Journal of Computational and Theoretical Nanoscience* **2018**, *15*, 470–473, https://doi.org/10.1166/jctn.2018.7113.
28. Abdelsalam, H.; Elhaes, H.; Ibrahim, M.A. First principles study of edge carboxylated graphene quantum dots. *Physica B* **2018**, *537*, 77-86, https://doi.org/10.1016/j.physb.2018.02.001.
29. Abdelsalam, H.; Saroka, V.A.; Ali, M.; Teleb, N.H.; Elhaes, H.; Ibrahim, M.A. Stability and electronic properties of edge functionalized silicene quantum dots: A first principles study. *Physica E: Low-dimensional Systems and Nanostructures* **2019**, *108*, 339–346, https://doi.org/10.1016/j.physe.2018.07.022.
30. Gaussian 09, Revision C.01, Frisch, M.J.; Trucks, G.W.; Schlegel, H.B.; Scuseri, G.E.; Robb, M.A.; Cheeseman, J.R.; Scalmani, G.; Barone, V.; Mennucci, P.B.G.A.; Nakatsuji, H.; Caricato, M.; Li, X.; Hratchain, P.H.; Izmaylov, A.F.; Bloino, J.; Zheng, G.; Sonnenberg, J.L.; Hada, M.; Ehara, M.; Toyota, K.; Fukuda, R.; Hasegawa, J.; Ishida, M.; Nakajima, T.; Honda, Y.; Kitao, O.; Nakai, H.; Vreven, T.; Montgomery, J.A.; Jr, Peralta, J.E.; Ogliaro, F.; Bearpark, M.; Heyd, J.J.; Brothers, E.; Kudin, K.N.; Staroverov, V.N.; Keith, T.; Kobayashi, R.; Normand, J.; Raghavachari, K.; Rendell, A.; Burant, J.C.; Iyengar, S.S.; Tomasi, J.; Cossi, M.; Rega, N.; Millam, J.M.; Klene, M.; Knox, J.E.; Cross, J.B.; Bakken, V.; Adamo, C.; Jaramillo, J.; Gomperts, R.; Stratmann, R.E.; Yazyev, O.; Austin, A.J.; Cammi, R.; Pomelli, C.; Ochterski, J.W.; Martin, R.L.; Morokuma, K.; Zakrzewski, V.G.; Voth, G.A.; Salvador, P.; Dannenberg, J.J.; Dapprich, S.; Daniels, A.D.; Farkas, O.; Foresman, J.B.; Ortiz, J.V.; Cioslowski, J.; Fox, D.J. Gaussian, Inc., Wallingford CT **2010**.
31. Becke, A.D. Density functional thermochemistry. III. The role of exact exchange. *Chem. Phys.* **1993**, *98*, 5648, https://doi.org/10.1063/1.464913.
32. Lee, C.; Yang, W.; Parr, R.G. Development of the Colle-Salvetti correlation-energy formula into a functional of the electron density. *Physical Review B* **1988**, *37*, 785.
33. Miehlich, B.; Savin, A.; Stoll, H.; Preuss, H. Results obtained with the correlation energy density functionals of becke and Lee, Yang and Parr. *Chemical Physics Letters* **1989**, *157*, 200, https://doi.org/10.1016/0009-2614(89)87234-3.